Chemistry & Biology
Article

Expanded Polyglutamine-Binding Peptoid as a Novel Therapeutic Agent for Treatment of Huntington's Disease

Xuesong Chen,[1] Jun Wu,[1] Yuan Luo,[1] Xia Liang,[1] Charlene Supnet,[1] Mee Whi Kim,[1] Gregor P. Lotz,[2] Guocheng Yang,[2] Paul J. Muchowski,[2,3] Thomas Kodadek,[4] and Ilya Bezprozvanny[1,*]
[1]Department of Physiology, University of Texas Southwestern Medical Center at Dallas, Dallas, TX 75390, USA
[2]Gladstone Institute of Neurological Diseases
[3]Departments of Biochemistry and Biophysics and of Neurology
University of California, San Francisco, San Francisco, CA, USA
[4]The Scripps Research Institute, Jupiter, FL, USA
*Correspondence: Ilya.Bezprozvanny@UTSouthwestern.edu
DOI 10.1016/j.chembiol.2011.06.010

SUMMARY

Polyglutamine(polyQ)-expanded proteins are potential therapeutic targets for the treatment of polyQ expansion disorders such as Huntington's disease (HD) and spinocerebellar ataxia type 3 (SCA3). Here, we used an amino-terminal fragment of a mutant Huntingtin protein (Htt-N-82Q) as bait in an unbiased screen of a 60,000 peptoid library. Peptoid HQP09 was selected from the isolated hits and confirmed as a specific ligand of Htt-N-82Q and Atxn3-77Q mutant proteins in biochemical experiments. We identified three critical residues in the HQP09 sequence that are important for its activity and generated a minimal derivative, HQP09_9, which maintains the specific polyQ-binding activity. We demonstrated that HQP09 and HQP09_9 inhibited aggregation of Htt-N-53Q in vitro and exerted Ca^{2+}-stabilizing and neuroprotective effects in experiments with primary striatal neuronal cultures derived from HD mice. We further demonstrated that intracerebroventricular delivery of HQP09 to an HD mouse model resulted in reduced accumulation of mutant Huntingtin aggregates and improved motor behavioral outcomes. These results suggest that HQP09 and similar peptoids hold promise as novel therapeutics for developing treatments for HD, SCA3, and other polyglutamine expansion disorders.

INTRODUCTION

The abnormal expansion of polyglutamine (polyQ) tracks in the coding sequences of several proteins causes misfolding of these proteins and initiates neurodegenerative diseases including Huntington's disease (HD), spinocerebellar ataxia type 3 (SCA3), and several other related disorders (Gusella and MacDonald, 2000; The Huntington's Disease Collaborative Research Group, 1993). Polyglutamine expansions longer than 35Q in the context of Huntingtin (Htt) or ataxin-3 (Atxn3) proteins result in HD and SCA3, respectively. The neuropathological hallmark of HD is the selective degeneration of medium spiny neurons (MSNs) in the striatum (caudate nucleus and putamen) (Vonsattel and DiFiglia, 1998; Vonsattel et al., 1985). The brain regions most affected in SCA3 are the dentate and pontine nuclei, internal portion of globus pallidus, subthalamic nucleus, substantia nigra (SN), and spinocerebellar tracts (Stevanin et al., 2000). Polyglutamine-expanded proteins are prone to form aggregates and nuclear inclusions, which may be toxic to neurons (Shao and Diamond, 2007). However, the exact mechanism(s) responsible for such toxicity are unknown. These proteins are involved in a number of pathological interactions with signaling proteins in cells, causing abnormalities in transcription, proteosomal and mitochondrial functions, Ca^{2+} signaling, and other essential cellular functions. One potential therapeutic approach is to target these downstream signaling pathways and to correct signaling abnormalities induced by the expression of polyQ-expanded proteins. Such an approach has been extensively discussed for transcriptional, mitochondrial, and Ca^{2+} signaling pathways (Benn et al., 2008; Bezprozvanny, 2009; Chaturvedi and Beal, 2008).

An alternative strategy is to target the mutant polyQ-expanded mutant protein itself and prevent the detrimental downstream signaling altogether. The silencing of mutant Htt (mHtt) by RNAi-encoding viruses resulted in the improved behavioral and neuropathological abnormalities in a mouse model of HD (Harper et al., 2005). Likewise, viral delivery of short hairpin RNAs specific for mutant ataxin-1 (mAtxn1) resolved characteristic Purkinje cell inclusions, restored cellular morphology, and profoundly improved motor coordination in SCA type 1 mice (Xia et al., 2004). Recently, the selective knockdown of mRNA encoding mHtt and mAtxn3 proteins has been demonstrated using peptide nucleic acid (PNA) and locked nucleic acid (LNA) antisense oligomers targeting expanded CAG repeat (Hu et al., 2009). These antisense oligomers effectively silence the mutant mRNA while leaving wild-type (WT) Htt and Atxn3 mRNA levels intact (Hu et al., 2009).

Another potential therapeutic strategy would be to target the mutant proteins directly by inhibiting their ability to form toxic aggregates. Proteins containing polyQ expansions can exist in multiple conformations, some of which are innocuous and some of which are aggregation-prone and toxic (Shao and

Diamond, 2007). For example, it has been shown that an increase in chaperone levels can shift the balance away from toxic conformations of polyQ-expanded proteins and reduce toxicity (Wacker et al., 2004; Warrick et al., 1999; Wyttenbach et al., 2002). Intrabodies developed against an epitope of human Htt reduced the specific neurotoxicity of mHtt by preventing its accumulation in neuronal processes and promoting its clearance from the cytoplasm (Colby et al., 2004; Khoshnan et al., 2002; Lecerf et al., 2001; Wolfgang et al., 2005). Furthermore, a specific polyQ binding peptide (QBP1), identified from a combinatorial peptide library expressed on M13 phage pIII protein (Nagai et al., 2000), has been reported to prevent the toxic conformational transition within polyQ-expanded proteins (Nagai et al., 2000) and exert neuroprotective effects in cellular and fly models of polyQ toxicity (Nagai et al., 2003; Popiel et al., 2007, 2009). Several small molecules have been isolated in screens as inhibitors of polyQ aggregation and some were able to reduce polyQ aggregation and toxicity in cellular and animal models (Chopra et al., 2007; Ehrnhoefer et al., 2006; Heiser et al., 2002; Sánchez et al., 2003; Wang et al., 2005; Zhang et al., 2005). However, none of these small-molecule candidates have successfully advanced into clinical trials because of problems in finding an appropriate mode of delivery, poor pharmacokinetics, and low efficacy in vivo.

The goal of the present study was to identify a polyQ-binding small molecule with "drug-like" properties that would have the potential to inhibit the formation of toxic protein aggregates. The approach was to take advantage of an efficient peptoid library synthesis and screening technology. Peptoids (oligomers of N-substituted glycines) were developed as scaffolds for the generation of chemically diverse libraries of novel molecules (Simon et al., 1992) and they have been proven to be a rich source of specific ligands for many types of proteins, including several that have never before been targeted pharmacologically (Zuckermann and Kodadek, 2009). In the present study a one-bead-one-compound peptoid library was synthesized, containing 60,000 unique compounds. The generated library was screened for molecules that specifically bound an amino-terminal fragment of the mHtt protein (Htt-N-82Q) fused to maltose-binding protein (MBP). A peptoid called HQP09 was isolated in the screen and confirmed as a specific mHtt and mAtxn3 binding partner in biochemical experiments. A minimal derivative peptoid HQP09–9 was produced as a result of the structure-activity relationship analysis of HQP09. The actions of HQP09 and HQP09–9 were characterized in an in vitro aggregation assay with mHtt and in cellular toxicity assays with primary MSN cultures prepared from YAC128 mice. Furthermore, delivery of HQP09 by intracerebroventricular (ICV) injection decreases mHtt aggregation in YAC128 mice. These results argue that, in general, direct pharmacological blockade of polyQ aggregation is possible and that peptoids in particular hold promise as lead compounds for the development of drugs against HD, SCA3, and other polyQ-expansion disorders.

RESULTS

The Identification of Peptoid HQP09 from a Library as a Ligand for mHtt

To identify a mHtt-binding peptoid, we generated a bead-displayed peptoid library composed of 60,000 diverse 6-mer peptoids on TentaGel macrobeads (see Methods for details). In the general structure of the library (Figure 1A), a proline was fixed at the fourth position, whereas the other five positions were randomized using nine different primary amines (Figure 1B). The fixed proline residue was selected because proline has been reported to be essential for the association of the QBP1 peptide with polyQ-expanded proteins (Hamuro et al., 2007). A residue containing a hydroxyethyl side group was added between the 6-mer peptoid and the resin to provide a consistent residue to aid in mass spectrometry–based characterization and to increase solubility. Mutant Htt proteins that harbor more than 35 glutamine residues easily aggregate in vitro, but for screening purposes soluble mHtt is required. To address this issue, we generated a fusion protein between Htt-82Q amino-terminal and a MBP (MBP-Htt-N-82Q). For comparison, WT MBP-Htt-N-15Q protein was also expressed and purified. Both MBP-Htt-N-82Q and MBP-Htt-N-15Q proteins were monomeric and stable in solution (data not shown).

The MBP-Htt-N-82Q protein was used as bait to screen the 60,000 peptoid library using a recently developed beads-based screening method (Xiao et al., 2007). The beads were initially incubated with MBP-Htt-N-82Q protein and then beads with bound protein were visualized using anti-MBP mouse monoclonal antibodies and goat anti-mouse antibodies-coated red quantum dots (Qdots) (see Methods for details). The beads displaying potential hits were identified by the red halo (Qdot positive) visible on the bead surface under a fluorescence microscope at excitation wavelength of 410 nm (Figure 1C). Twenty such beads were picked using a micropipette. To eliminate beads that might bind the antibodies rather than the target protein, all proteins were stripped off the beads using SDS and probed again with biotinylated MBP-Htt-N-82Q protein and streptavidin-coated Qdots. Ten of the 20 beads were positive in the re-screening assay with biotinylated MBP-Htt-N-82Q protein, suggesting that they recognize MBP-Htt-N-82Q protein directly. The peptoids on these 10 beads were sequenced by Edman degradation and designated as HQPs (Huntingtin polyQ binding Peptoids). Because some of these peptoids had similar sequences (see Figure S1 available online), only five representative peptoids—HQP02, HQP04, HQP06, HQP07, and HQP09—were re-synthesized on TentaGel beads and evaluated in the Qdot binding experiments with MBP-Htt-N-82Q protein. No binding was detected for HQP02, HQP04, HQP06, or HQP07 beads. However, strong binding was detected for HQP09 beads (data not shown). The HQP09 beads also displayed significantly stronger binding to MBP-Htt-N-82Q than to MBP-Htt-N-15Q (data not shown). Thus, we selected HQP09 (Figure 2A) as a specific mHtt ligand for further evaluation.

HQP09 Specifically Binds to polyQ-Expanded Proteins In Vitro

In the next series of experiments, we evaluated the association between the peptoid HQP09 and mHtt using conventional biochemical binding assays. TentaGel beads displaying HQP09 were incubated with recombinant MBP-Htt-N-82Q or MBP-Htt-N-15Q proteins and precipitated by centrifugation. Attached proteins were resolved by gel electrophoresis and analyzed by western blotting with anti-MBP monoclonal antibodies. The

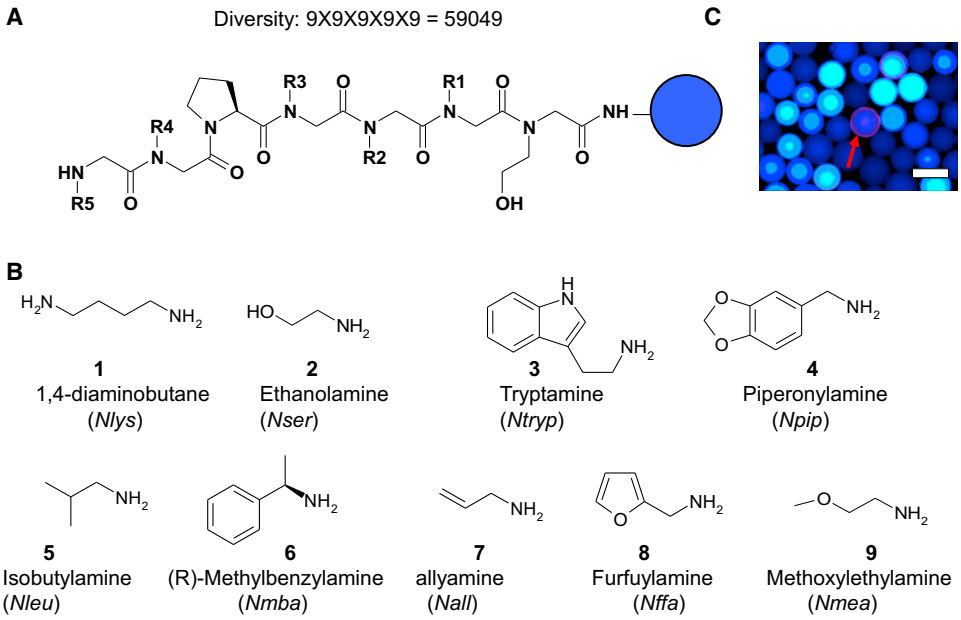

Figure 1. Peptoid Library Used in the Screen for Specific mHtt Ligands

(A) General chemical structure of the 6-mer peptoid library containing a fixed proline residue at the 4th position and 5 variable positions (R1-R5). The calculated diversity of the library is 59,049 diverse peptoids.

(B) Chemical structures and names of 9 amines used in synthesizing the peptoid library.

(C) A fluorescence microscopic image showing a representative hit isolated from the peptoid library as a potential ligand for MBP-Htt-N-82Q protein. The bead containing a putative hit (shown by the red arrow) is identified by a red halo around the bead resulting from Qdot fluorescence. Scale bar represents 170 μm. See also Figure S1.

TentaGel beads containing a random 6-mer peptoid RP01 (Figure 2A) were used as a negative control, whereas streptavidin-coated beads conjugated with biotinylated Bio-$(QBP1)_2$ tandem peptide (Nagai et al., 2000) were used as a positive control. Consistent with previous observations (Nagai et al., 2000), Bio-$(QBP1)_2$ beads retained about 50% of the input MBP-Htt-N-82Q but only a trace amount of MBP-Htt-N-15Q (Figure 2B). The HQP09 beads retained about 40% of the input MBP-Htt-N-82Q but none of the MBP-Htt-N-15Q (Figure 2B). Control RP01 beads did not associate with either protein (Figure 2B). These data suggested that HQP09 specifically bound expanded mHtt protein and that HQP09 peptoid and Bio-$(QBP1)_2$ peptide bound mHtt with similar affinities.

Is HQP09 specific for mHtt or does it bind to other polyQ-expanded proteins as well? To answer this question, we performed pull-down experiments using HQP09 beads incubated with full length WT Atxn3-19Q and mutant Atxn3-77Q. The precipitated proteins were detected by western blotting with an anti-Atxn3 monoclonal antibody. The data show that HQP09 beads bind to Atxn3-77Q protein more efficiently than to Atxn3-19Q protein (Figure 2C). The control beads coated with the RP01 peptoid did not bind either protein (Figure 2C). The beads attached to Bio-$(QBP1)_2$ peptide precipitated similar amounts of Atxn3-77Q and Atxn3-19Q proteins (Figure 2C). From these results we concluded that HQP09 peptoid bound to multiple polyQ-expanded proteins and that the specificity of HQP09 for an expanded polyQ track was comparable with, or better than, the specificity of the Bio-$(QBP1)_2$ peptide.

To obtain greater insight into the binding of HQP09 to mHtt, we performed a series of competitive binding experiments. In these experiments, QBP1 peptide (at 100 μM or 300 μM), HQP09 peptoid (300 μM), or control RP01 peptoid (300 μM) were included in the binding reaction between HQP09-displaying beads and MBP-Htt-N-82Q protein. The peptoid-bound proteins were analyzed by western blotting with anti-MBP monoclonal antibodies. We found that the addition of soluble HQP09 peptoid reduced the fraction of precipitated MBP-Htt-N-82Q protein, but the addition of control RP01 peptoid or QBP1 peptide had no effect (Figure 2D). In reverse experiments, we determined that QBP1 peptide, but not HQP09 or RP01 peptoids, reduced the fraction of MBP-Htt-N-82Q protein bound by QBP1 peptide-displaying beads (Figure 2E). Taken together (Figure 2D, 2E), these results suggest that HQP09 and QBP1 do not compete with each other, but rather bind to non-overlapping sites on the MBP-Htt-N-82Q protein. Consistent with previous observations (Figures 2B and 2C), we confirmed that HQP09 was selective for mutant MBP-Htt-N-82Q protein (Figure 2D), whereas QBP1-displaying beads associated with the WT MBP-Htt-N-15Q protein to a significant degree (Figure 2E).

Structure-Activity Analysis of HQP09

To determine the affinity of the HQP09 association with mHtt in solution, we developed a solution phase fluorescence polarization (FP) assay between fluorescein-labeled HQP09 (HQP09_G2_Fluo) (Figure 3A) and MBP-Htt-N-82Q. The association of HQP09_G2_Fluo with the target protein leads to a reduction in the rotational mobility of the fluorescein label, which could

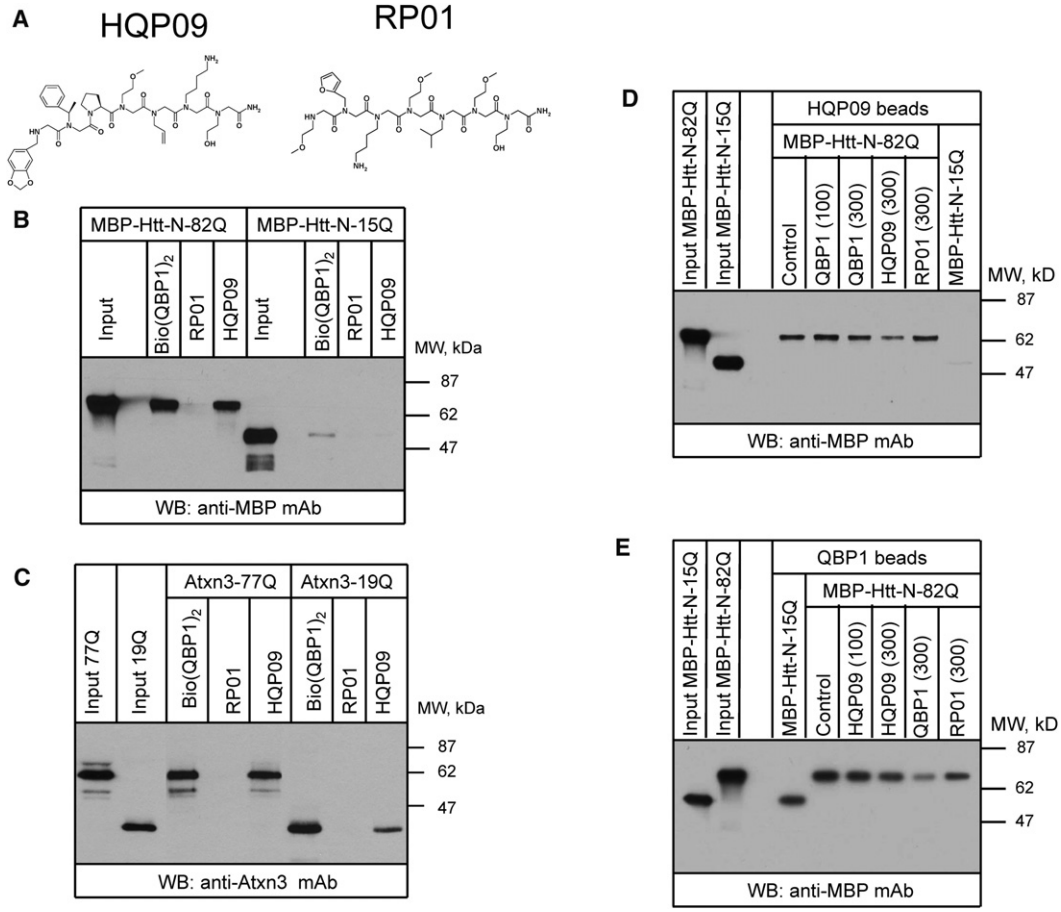

Figure 2. HQP09 Peptoid Specifically Binds to polyQ-Expanded Proteins

(A) Chemical structure of HQP09 peptoid identified from the screen of the peptoid library. RP01 is a random 6-mer peptoid used as a negative control.

(B) MBP-Htt-N-82Q or MBP-Htt-N-15Q recombinant proteins were used in pull-down experiments with bio-$(QBP1)_2$, HQP09 or RP01 beads. The precipitated fractions were analyzed by western blotting with anti-MBP monoclonal antibodies.

(C) Atxn3-77Q or Atxn3-19Q recombinant proteins were used in pull-down experiments with bio-$(QBP1)_2$, HQP09, or RP01 beads. The precipitated fractions were analyzed by western blotting with anti-Atxn3 monoclonal antibodies.

(D and E) MBP-Htt-N-82Q and MBP-Htt-N-15Q recombinant proteins were used in pull-down experiments with HQP09 beads (D) or QBP1 beads (E). The QBP1 peptide, HQP09 peptoid, or RP01 peptoid were added in binding reaction as indicated. The precipitated fractions were analyzed by western blotting with an anti-MBP monoclonal antibody.

On (A–E), the input lane contained 1% of total protein used in pull-down experiments.

be quantified as an increase in FP values (Δmp). In our experiments, 5 nM of HQP09_G2_Fluo was incubated with increasing concentrations of MBP-Htt-N-82Q in the presence of 1.0 μM bovine serum albumin (BSA). The results were consistent with a K_d value of 12 μM for the association between HQP09_G2_Fluo and MBP-Htt-N-82Q (Figure 3B). A control titration experiment using HQP09_G2_Fluo and BSA alone showed no apparent association (Figure 3B). The FP-quantified binding of HQP09_G2_Fluo to MBP-Htt-N-82Q was outcompeted in the presence of 300 μM of the parental peptoid HQP09 but not in the presence of 300 μM of the control peptoid RP01 (Figure 3C). These data confirmed that HQP09 specifically bound to MBP-Htt-N-82Q in solution.

In the next series of experiments, we took advantage of FP-based binding assays to identify the structural determinants responsible for association of HQP09 with mHtt. Our first aim was to define the minimum pharmacophore responsible for the HQP09 binding activity. For that purpose, we used sarcosine scanning, a method that we have recently applied successfully to identifying the minimum pharmacophore of a peptoid antagonist of VEGFR2 (Udugamasooriya et al., 2008b). A series of sarcosine scanning derivatives was obtained by replacing one of the seven residues in HQP09 (Figure 3A, positions 1–7) with a sarcosine. The corresponding seven peptoids (HQP09_1 to HQP09_7, Figure S2) were synthesized and used at a concentration of 300 μM in competitive FP binding assays with HQP09_G2_Fluo and MBP-Htt-N-82Q. We found that HQP09_1 and HQP09_2 had no effect on FP signal and that HQP09_4 reduced FP signal by 50% (Figure 3C). HQP09_3, HQP09_5, HQP09_6, and HQP09_7 were as potent as HQP09 itself and reduced FP signal by more than 75% (Figure 3C). These data suggested that three of the seven residues of HQP09—1

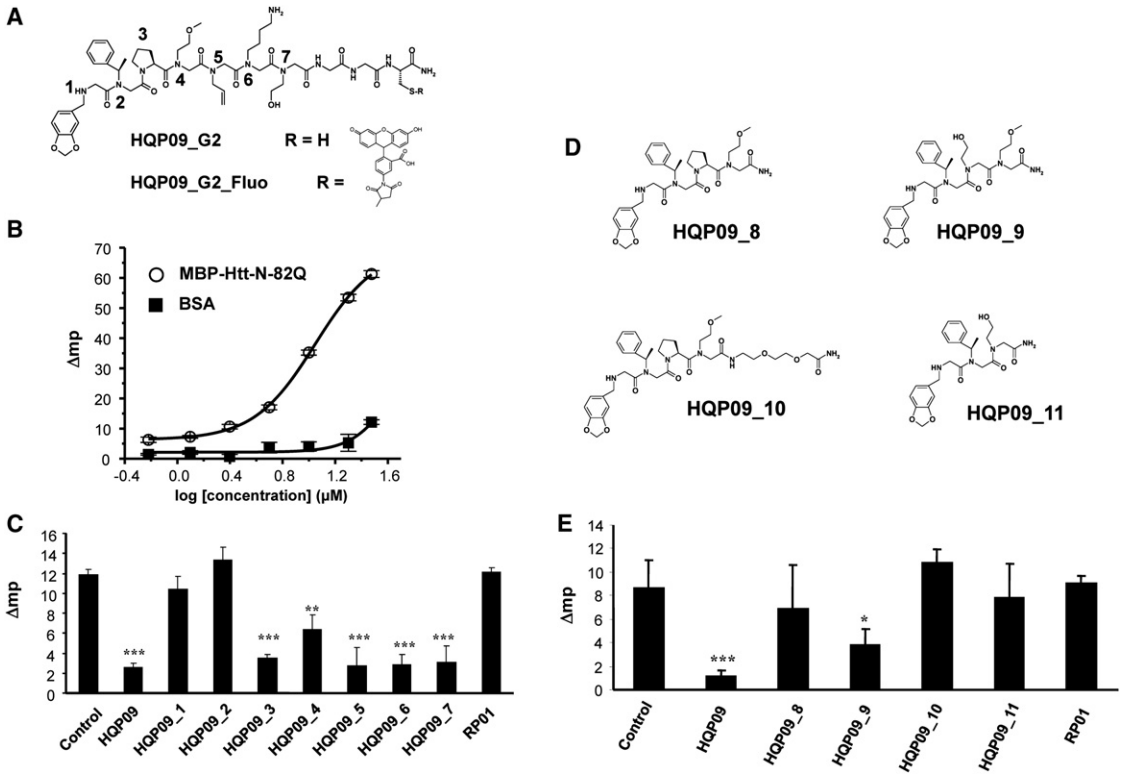

Figure 3. Structure-Activity Studies of HQP09 using Fluorescence Polarization mHtt-Binding Assay

(A) Chemical structures of HQP09_G2 and HQP09_G2_Fluo.

(B) Fluorescence polarization assay. 5 nM of HQP09_G2_Fluo was incubated with indicated amounts of BSA or MBP-Htt-N-82Q protein in 1 μM BSA. The fluorescence polarization values (Δmp) are shown at each protein concentration as mean ± SE (n = 3) for BSA (filled squares) or MBP-Htt-N-82Q (open circles). The fit to the titration curve (smooth line) yielded apparent kd ≈12 μM for MBP-Htt-N-82Q association with HQP09.

(C) Competitive fluorescence polarization assay. HQP09 peptoid, RP01 peptoid or the seven sarcosine scan derivatives of HQP09 as indicated were added in a final concentration of 300 μM to a binding assay between 5 nM HQP09_G2_Fluo and 5 μM MBP-Htt-N-82Q. The fluorescence polarization values (Δmp) measured in the absence (con) or presence of each peptoid are shown as mean ± SE (n = 3). The significant reduction in Δmp values when compared with control is shown (***$p < 0.001$, **$p < 0.01$).

(D) Chemical structures of four 4-mer HQP09 analogs.

(E) Results of competitive fluorescence polarization assay performed with HQP09, 4-mer HQP09 analogs, and RP01 (300 μM each). The assay was performed as described in (C) and Δmp values presented as mean ± SE (n = 3). HQP09 and HQP09_9 significantly reduced measured Δmp values when compared with control (***$p < 0.001$, *$p < 0.05$). Other 4-mer analogs had no significant effect ($p > 0.05$).

See also Figure S2 and Table S1.

(Npip), 2 (Nmba), and 4 (Nmea) (Figures 1B and 3A)—constituted a minimal pharmacophore important for the association of the peptoid with MBP-Htt-N-82Q, where positions 1 (Npip) and 2 (Nmba) play a predominant role.

With this information, we aimed at generating a minimally active derivative of HQP09. We reasoned that a smaller molecule would be more advantageous for biological assays and have better potential as a lead for drug development. To achieve this goal, we synthesized four peptoid derivatives of HQP09 named HQP09_8, HQP09_9, HQP09_10, and HQP09_11 (Figure 3D). The activities of these peptoid derivatives were tested at 300 μM in competitive FP assays with HQP09_G2_Fluo and MBP-Htt-N-82Q. We found that HQP09_9 inhibited FP signal by more than 50%, HQP09_8 was modestly effective, and HQP09_10 and HQP09_11 were ineffective (Figure 3E). Although HQP09_9 was less effective than HQP09 (Figure 3E), the molecular weight of HQP09_9 (MW = 585) was 1.6-fold lower than the molecular weight of HQP09 (MW = 908). Thus, we selected HQP09_9 as the lead HQP09 derivative for cell-based assay evaluation.

PolyQ-Binding Peptoids Inhibit mHtt Aggregation In Vitro

Polyglutamine-expanded proteins are prone to aggregation, and aggregation of mHtt may contribute to its toxicity (Shao and Diamond, 2007). We aimed to evaluate the anti-aggregation activities of HQP09 and HQP09_9 peptoids using an in vitro aggregation assay of mHtt as previously described (Wacker et al., 2004). The random peptoid RP01 and inactive analog HQP09_01 (Figure S2) were used as controls to verify the specificity of the observed effects, and the polyQ-binding peptide QBP1 (Nagai et al., 2000) was used as a positive control for anti-aggregation activities. The first exon of Htt-53Q protein was expressed in bacteria as a glutathione *S*-transferase (GST) fusion protein and purified as previously described (Wacker

et al., 2004). After purification, GST-Htt53Q appeared non-aggregated by the atomic force microscopy (AFM) analysis and by size-exclusion chromatography (data not shown). Cleavage of a unique peptide sequence between the GST moiety and Htt53Q with a site-specific protease releases the Htt53Q fragment, initiating aggregation in a time-dependent manner (Wacker et al., 2004). To measure the degree of Htt53Q aggregation we used a filter trap assay in which detergent-insoluble mHtt aggregates were detected by the anti-Htt MW8 antibody (Wacker et al., 2004). Large amounts of trapped Htt53Q aggregates were detected in samples collected 24 hr after cleavage from GST (Figure 4A). The addition of 10 μM QBP1 peptide inhibited Htt53Q aggregation by 40% (Figure 4A), consistent with published results (Nagai et al., 2007). When tested with the same concentration (10 μM), HQP09 peptoid inhibited Htt53Q aggregation by 80%, significantly better than QBP1 peptide (Figure 4A). The HQP09_9 derivative inhibited Htt53Q aggregation by 30%, not significantly different from the QBP1 peptide (Figure 4A). The control peptoids RP01 and HQP09_1 were not effective in preventing Htt53Q aggregation (Figure 4A). In addition to the filter trap assay, the formation of Htt53Q aggregates was also evaluated by SDS-PAGE gel followed by western blotting with MW8 antibody. When analyzed by SDS-PAGE assay performed after 24 hr incubation, we found that the HQP09 peptoid and QBP1 peptide effectively reduced the formation of mHtt aggregates, HQP09_9 peptoid was partially effective, and RP01 and HQP09_1 peptoids had no effect (Figure S3A).

To further characterize the inhibition of Htt53Q aggregation by HQP09 and HQP09_09, we used atomic force microscopy (AFM) to image the structures of aggregates (oligomers or fibrils) in solution. Before AFM imaging, samples of Htt53Q solution taken after the 24 hr incubation were diluted 20 times so as to clearly image individual fibrils or oligomers on the surface. Large fibrils and oligomers were observed in control AFM experiments when Htt53Q was incubated with 3% DMSO (Figure 4B). Formation of the AFM-visible fibrils and oligomers was abolished in the presence of QBP1 peptide, HQP09 peptoid, or HQP09_9 peptoid (Figure 4B). In contrast, a large number of fibrils and oligomers were observed in the presence of RP01 or HQP09_1 peptoids (Figure 4B). Quantification of the number of observed particles larger than 100 nm, as analyzed by AFM, is shown on Figure S3B. Overall, results from the filter trap assay, SDS-PAGE, and AFM imaging experiments indicated that HQP09 and HQP09_9 peptoids were highly effective in inhibiting mHtt aggregation. The abilities of HQP09 and HQP09_9 to inhibit mHtt aggregation were comparable with the activity of the previously identified QBP1 peptide (Nagai et al., 2000) and the anti-aggregation effects of the peptoids were specific, because random peptoid RP01 and the inactive derivative HQP09_01 had no such effect in any of these aggregation assays.

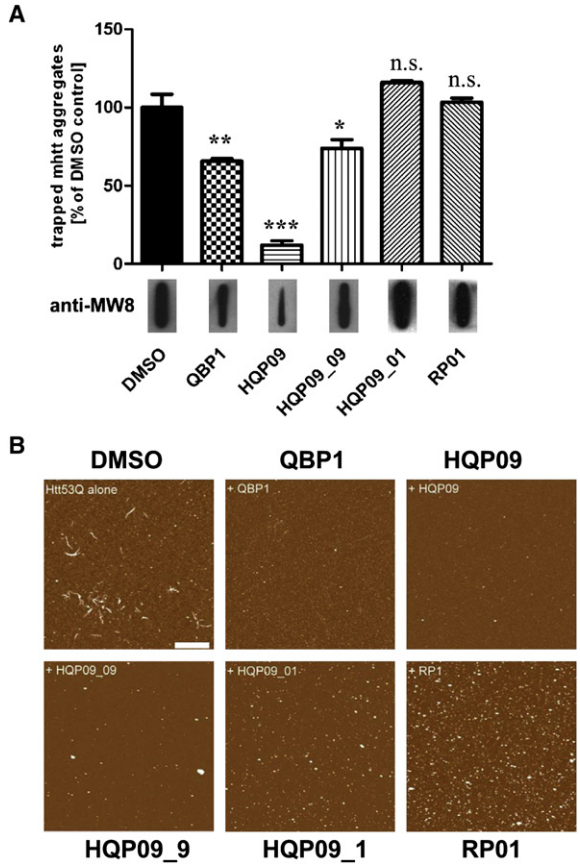

Figure 4. PolyQ-Binding Peptoids Inhibit mHtt Aggregation

(A) Filter trap assay. The Htt53Q aggregates formed after 24 hr incubation were trapped and detected by MW8 antibodies. The aggregation reaction was performed in the presence of 3% DMSO, QBP1 peptide, HQP09, HQP09_9, HQP09_1, or RP01 peptoids (10 μM each) as indicated. The amounts of Htt53Q aggregates were quantified by using densitometry of MW8 signals and normalized to the signal observed in DMSO control in the same experiment. The averaged and normalized results are presented as mean ± SE (n = 3 independent experiments).

(B) AFM images of Htt53Q aggregates formed after 24 hr incubation in the presence of 3% DMSO, QBP1 peptide, HQP09, HQP09_9, HQP09_1, or RP01 peptoids (10 μM each) as indicated. The particles corresponding to fibrils and oligomers formed by Htt53Q are clearly visible in DMSO control (top left) and in the presence of HQP09_1 (bottom center) or RP01 (bottom right). The number of particles is reduced in the presence of QBP1 (top center), HQP09 (top right), and HQP09_9 (bottom left).

Scale bar represents 2 μm for all panels. Quantification of the number of particles over 100 nm detected on these images is shown as Figure S3B.

PolyQ-Binding Peptoids Stabilize Glutamate-Induced Ca^{2+} Signaling in YAC128 MSN

Mutant Htt binds to a number of Ca^{2+} channels and signaling proteins, and deranged neuronal Ca^{2+} signaling plays an important role in HD pathogenesis (Bezprozvanny, 2009). In our previous studies, we found that repetitive pulses of 20 μM glutamate resulted in a larger elevation of cytosolic Ca^{2+} levels in YAC128 MSN when compared with WT MSN (Tang et al., 2005). Could HQP09 or HQP09_9 peptoids sequester mHtt and stabilize abnormal Ca^{2+} signals in HD MSN? To evaluate the biological activity of HQP09 or HQP09_9 peptoids, we performed Ca^{2+} imaging experiments with MSN cultures derived from WT and YAC128 mice preincubated with 20 μM HQP09 or HQP09_9 peptoids. Random peptoid RP01 was used in the same concentration (20 μM) as a control for the specificity of the observed effects. The peptoids were added to the culture media at day in vitro (DIV)1 and DIV13 to allow sufficient time for binding mHtt, and Ca^{2+} imaging experiments were performed at DIV13 as previously described (Tang et al., 2005). The

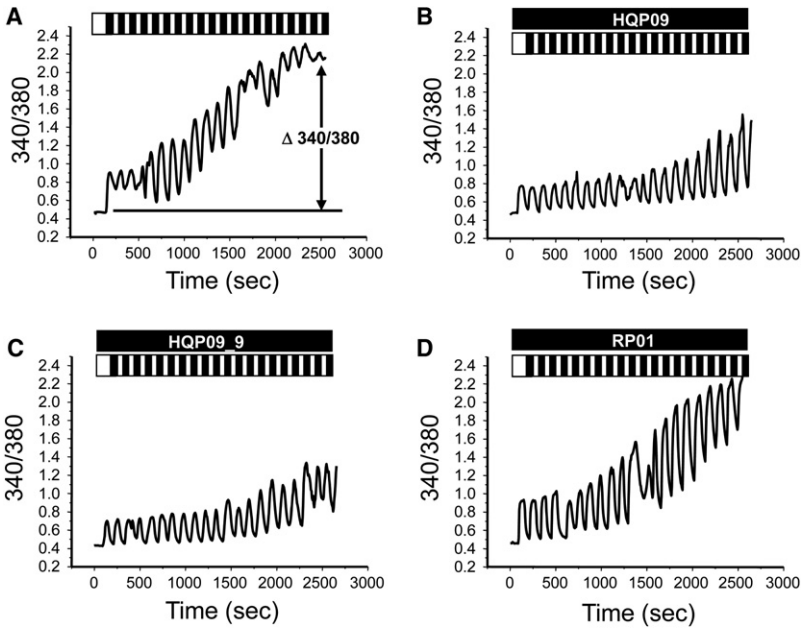

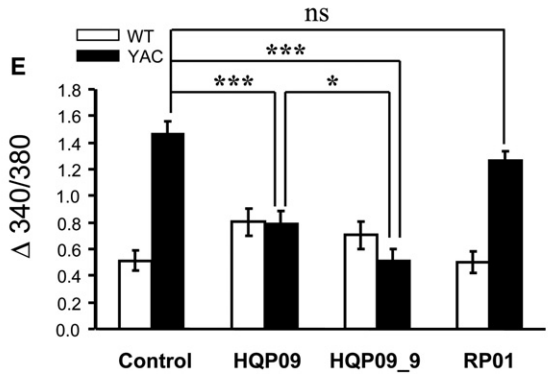

Figure 5. PolyQ-Binding Peptoids Stabilize Glutamate-Induced Ca^{2+} Signals in HD-YAC128 MSN

(A) Repetitive application of 20 μM glutamate (shown as black bars) induces enhanced Ca^{2+} signals in MSN cultures from HD-YAC128 mice. The intracellular Ca^{2+} concentration is measured by Fura-2 ratio imaging and presented as 340/380 Fura-2 ratio at each time point in the experiment.

(B–D) The same experiment as in panel (A) was performed after preincubation with 20 μM HQP9 (B), HQP9_9 (C), or RP01 (D). On (A–D), the representative trace from all HD-YAC128 MSN in each experimental group are shown.

(E) The summary of Ca^{2+} increase in WT (open column) and YAC128 (filled column) MSN after 20 pulses of glutamate. The average increase in Ca^{2+} levels is shown by change in 340/380 ratio as mean ± SE ($n \geq 33$ for the number of MSN analyzed in each group). Preincubation with HQP09 or HQP09_9 significantly (***$p < 0.001$) attenuated glutamate-induced Ca^{2+} responses in YAC128 MSN. HQP09_9 peptoid had significantly (*$p < 0.05$) stronger effect than HQP09. RP01 had no significant effect (ns) on YAC128 MSN Ca^{2+} signals.

intracellular neuronal Ca^{2+} concentration in these experiments was continuously monitored by Fura-2 imaging and the 340/380 ratio was used to quantify Ca^{2+} levels. In agreement with our previous findings (Tang et al., 2005, 2007), the increase in Ca^{2+} levels after 20 pulses of 20 μM glutamate was significantly higher in YAC128 MSN than in WT MSN (Figures 5A and 5E). The glutamate-induced Ca^{2+} increase in YAC128 MSN cultures was significantly reduced by the addition of HQP09 or HQP09_9 peptoids (Figures 5B, 5C, and 5E). In contrast, RP01 had no effect on glutamate-induced Ca^{2+} signals in YAC128 MSN (Figure 5D, E). The effects of HQP09 and HQP09_9 were specific for YAC128 MSN and the addition of these peptoids did not have any significant effect on glutamate-induced Ca^{2+} signals in WT MSN (Figure 5E) or on basal Ca^{2+} levels (data not shown). HQP09_9 appeared to be the more effective "Ca^{2+} stabilizer" compared with HQP09 (Figure 5E), most likely because of the increased membrane permeability of the small derivative.

PolyQ-Binding Peptoids Are Neuroprotective in Cellular HD Model

The polyQ-binding peptoids prevent mHtt aggregation (Figure 4; Figure S3) and stabilize abnormal Ca^{2+} signals in YAC128 MSN (Figure 5). These results suggested that polyQ-binding peptoids could sequester mHtt and potentially reduce its toxicity. To evaluate the potential neuroprotective effects of polyQ-binding peptoids, we took advantage of the glutamate toxicity assay with YAC128 MSN cultures that we previously developed and have used extensively in testing potential HD neuroprotective agents (Hu et al., 2009; Tang et al., 2005, 2007, 2009; Wu et al., 2006, 2008, 2009, 2011). As in the Ca^{2+} imaging experiments, HQP09, HQP09_9, or RP01 (20 μM each) were added to WT and YAC128 MSN cultures on DIV1 and DIV13. The apoptotic cell death of cultured MSN neurons was scored by TUNEL staining as we previously described (Tang et al., 2005). In basal conditions, approximately 5% of MSNs were apoptotic (TUNEL-positive) in all experimental groups (Figure 6B), indicating that peptoids were not toxic for the cultured neurons at the concentrations tested. Consistent with our previous studies (Tang et al., 2005; Wu et al., 2011), the addition of 250 μM glutamate for 8 hr increased the percentage of apoptotic neurons to 60%–70% in YAC128 MSN (Figures 6A and 6B), but only to 30% in WT MSN (Figures 6A and 6B). In the presence of HQP09 and HQP09_9, the percentage of apoptotic YAC128 neurons was reduced to 30% and 21% respectively, to similar levels as WT neurons (Figures 6A and 6B). The presence of RP01 had no significant effect on the glutamate-induced cells death of YAC128 MSN (Figures 6A and 6B). From these experiments, we concluded that HQP09 and HQP09_9 exerted significant and specific neuroprotective effects on the excitotoxic cell death of YAC128 MSNs. Consistent with Ca^{2+} imaging studies (Figure 5), HQP09_9 appeared to be more neuroprotective than HQP09 (Figure 6B), presumably because of its better membrane permeability.

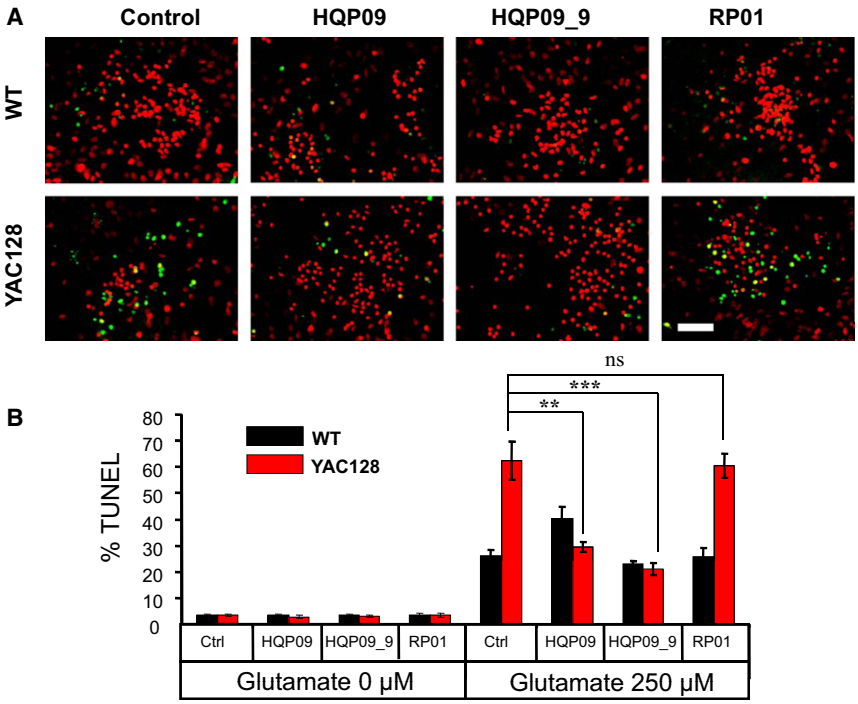

Figure 6. PolyQ-Binding Peptoids Protect HD-YAC128 MSN from Glutamate-Induced Apoptosis

(A) Representative images of TUNEL staining of MSN cultures from WT (top) and HD-YAC128 (bottom) mice. The MSN cultures were exposed to 250 μM glutamate for 8 hr, fixed, and analyzed by TUNEL staining (green) with propidium iodide counterstaining (red). Scale bar represents 40 μm. The images are shown for control cultures (first column), and for cultures preincubated with 20 μM of HQP09 (second column), HQP09_9 (third column), or RP01 (fourth column).

(B) The fraction of TUNEL-positive nuclei from WT (black bars) and HD-YAC128 (red bars) MSN cultures was calculated in the absence of glutamate stimulation and after 250 μM glutamate stimulation as indicated. The data are presented as mean ± SE (n = 6 microscopic fields, 200–300 MSNs per field). The fraction of TUNEL-positive YAC128 MSN nuclei was significantly (**$p < 0.01$, ***$p < 0.001$) reduced after preincubation with HQP09 and HQP09_9. Preincubation with RP01 had no significant effect (n.s.) on apoptosis of YAC128 MSN.

PolyQ-Binding Peptoids Inhibit the mHtt Aggregates in the Brain of YAC128 Mice

PolyQ-binding peptoids prevent the aggregation of mHtt 53Q proteins in vitro (Figure 4; Figure S3) and were neuroprotective in a cell toxicity assay using MSN cultures from YAC128 mice (Figure 6). To determine whether these peptoids had a protective effect in vivo, we decided to treat WT and YAC128 mice with peptoids and assess the impact of treatment on mHtt aggregation and stereotypic YAC128 behavior. In the previous studies, we used a similar in vivo approach to evaluate efficacy of potential HD therapeutic agents (Tang et al., 2007, 2009; Wang et al., 2010). The peptoid derivative HQP09_9 (20 mg/200 μl/mice, in saline) was delivered subcutaneously to YAC128 and WT mice using an Alzet osmotic pump for 8 months, beginning at the age of 3 months and replacing the pump every month. However, we did not observe a beneficial effect of HQP09_9 on the motor coordination of YAC128 mice compared with the control group, nor did we observe a decrease in the staining of mHtt aggregates in the striatum (data not shown). Most likely these negative results were related to poor blood-brain barrier permeability of HPQ09_9 (data not shown), so that therapeutic concentrations of HPQ09_9 have not been reached in striatum of YAC128 mice with subcutaneous delivery.

To bypass this problem, in the next series of experiments we used intracerebroventricular (ICV) infusion of peptoids using the Alzet osmotic pump (2.5 mg/100 μl/mice, in saline). In these experiments we also switched our focus to HQP09, which showed the strongest inhibition effect in the in vitro aggregation assay (Figure 4). In control experiments, we demonstrated that after one month of ICV infusion, the concentration of HQP09 in the brain was 100 times higher than in plasma (Table S2). Our data also demonstrate that HQP09 accumulated in the brain as the concentration of HQP09 after 21 days of infusion was significantly higher than it was after only 7 days (Table S2). To evaluate the therapeutic potential of HQP09, the ICV infusion experiments were initiated with 8–9-month-old WT and YAC128 mice. The performance of WT and YAC128 mice on the beam-walk test was recorded before and after 1 month ICV delivery of HQP09. In control experiments, WT and YAC128 mice of the same age were infused with carrier solution alone (ACSF). The ratio (performance after treatment/performance before treatment) of the beam-walk latency in the HQP09-treated group was better than in the ACSF control group and there was little effect of treatment on the two groups of WT mice (Figure S4). Importantly, both the area and intensity of mHtt aggregates significantly reduced in the striatum region of YAC128 brain after 30-day treatment with HQP09 when compared with the ACSF control group (Figures 7A–7C). These data suggest that HQP09 could inhibit mHtt aggregates in vivo, and the ability of HQP09 to accumulate in the brain may be one of the therapeutic advantages of peptoids in comparison to peptides. In control histological experiments, we confirmed that infusion with HQP09 peptoid did not result in toxicity to striatal neurons when compared with ACSF infusion (Figure S5).

DISCUSSION

Polyglutamine-expanded proteins adopt aggregate conformations that lead to pathological interactions with signaling proteins in cells (Shao and Diamond, 2007). Thus, specific polyQ-binding ligands have an obvious therapeutic potential for the treatment of HD and other polyQ-expanded disorders. A number of approaches have been attempted previously to identify specific polyQ-binding ligands. Intrabodies developed against an epitope of human Htt specifically bind to mHtt and reduce its toxicity in cellular and animal models (Colby et al., 2004;

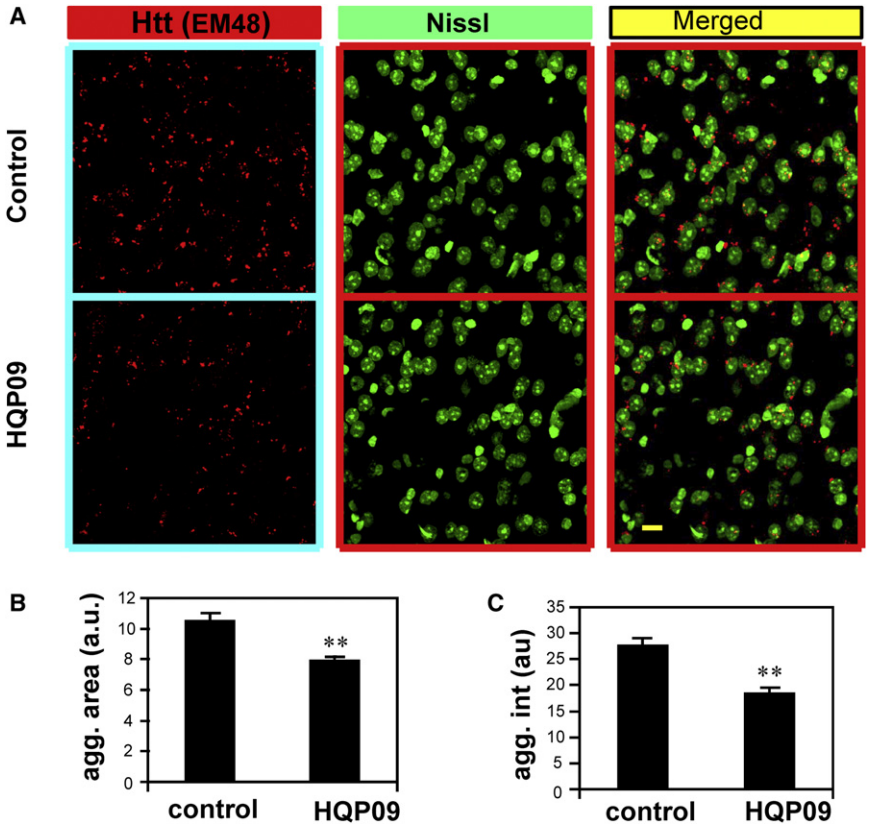

Figure 7. PolyQ-Binding Peptoid Inhibits mHtt Aggregates in YAC128 Mice

(A) Representative confocal images of the striatum region of brain slices showing mHtt aggregates (red) stained with EM48 antibody and nuclei stained with Nissl stain (green) from ACSF-treated (control, top) or HQP09-treated (HQP09, bottom) YAC128 mice. ACSF (100 μl/mice) or HQP09 (2.5 mg/100 μl/mice) was delivered by ICV using an Alzet osmotic pump for 30 days. Scale bar: 10 μm.

(B) The total mHtt aggregates area was quantified using MetaXpress from the striatum images of control (treated with ACSF) and HQP09-treated mice. The mean from 15 images per mouse are shown. The data are presented as mean ± SE (n = 4 for YAC128 control group and n = 3 for YAC128 HQP09 group, **p < 0.01).

(C) The total mHtt aggregates intensity was quantified using MetaXpress from the striatum images of control (treated with ACSF) and HQP09-treated mice. The mean from 15 images per mouse were used. The data are presented as mean ± SE (n = 4 for YAC128 control group and n = 3 for YAC128 HQP09 group, **p < 0.01).

See also Figures S4 and S5 and Table S2.

Khoshnan et al., 2002; Lecerf et al., 2001; Wang et al., 2008; Wolfgang et al., 2005). However, the therapeutic potential of intrabodies is limited by the requirement of viral delivery. A specific polyQ binding peptide (QBP1) was isolated in a phage library screen (Nagai et al., 2000). When coupled with a protein transduction domain (PTD), QBP1 suppressed polyQ-induced neurodegeneration in cultured cells and in a *Drosophila* model (Popiel et al., 2007). However, the benefit of long-term administration of PTD-QBP1 in a mouse model of HD was limited to weight loss phenotype (Popiel et al., 2009), which was most likely caused by low efficiency of PTD-QBP1 delivery to the brain after intraperitoneal administration (Popiel et al., 2009). A number of small molecules have been identified and isolated in screens as inhibitors of polyQ aggregation. Some of these molecules were able to reduce polyQ aggregation and toxicity in cellular and animal models (Chopra et al., 2007; Ehrnhoefer et al., 2006; Heiser et al., 2002; Sánchez et al., 2003; Wang et al., 2005; Zhang et al., 2005). However, these molecules showed very limited benefit in preclinical studies and none have advanced to clinical trials so far.

Here, we took advantage of a novel peptoid technology to identify and optimize a selective polyQ-binding ligand. Compared to peptides, peptoids are more resistant to protease degradation, more cell-permeable, more cost-effective, more readily synthesized, and can have higher structural diversities (Simon et al., 1992). Because of these favorable properties, peptoid libraries constitute rich sources of protein-binding ligands that have in vitro and in vivo biological functions (Zuckermann and Kodadek, 2009). Previously, peptoid technology was used to identify specific inhibitors of VEGF receptors (Udugamasooriya et al., 2008a), proteosome inhibitors (Lim et al., 2007), mimics of transcriptional activation domains (Liu et al., 2005; Xiao et al., 2007), other protein-binding ligands (Alluri et al., 2003, 2006; Simpson et al., 2009) and to isolate diagnostically useful antibodies in a sera collected from Alzheimer's patients (Reddy et al., 2011). This technology is particularly advantageous for developing inhibitors of protein-protein interactions, which are notoriously difficult to target using small molecules (Hershberger et al., 2007). For example, structure-based design was recently used to develop a peptoid that blocked the interactions between human double minute 2 (HDM2) protein and p53, an important target for cancer therapeutics (Hara et al., 2006). In the present study, we used an unbiased approach of screening a 6-mer peptoid library to isolate a peptoid HQP09 (MW = 908) that specifically bound to polyQ-expanded forms of mHtt and mAtx3 (Figure 2). By performing structure-activity analysis, we generated a minimal 4-mer derivative HQP09_9 (MW = 585) (Figure 3). Both HQP09 and HQP09_9 prevented aggregation of mHtt in vitro (Figure 4; Figure S3). The binding specificity and anti-aggregation activity of HQP09 were comparable with those of QBP1 peptide (Figures 2, 4 and Figure S3). Interestingly, HQP09 and QBP1 appeared to bind to non-overlapping sites on expanded polyQ sequence and did not compete with each other (Figure 2). Importantly, both HQP09 and HQP09_9 stabilized abnormal glutamate-induced Ca^{2+} signals in YAC128 MSN cultures (Figure 5) and protected YAC128 MSN from glutamate-induced apoptosis in vitro (Figure 6). HQP09_9 displayed more potent Ca^{2+} stabilizing and neuroprotection activities than HQP09 (Figures 5 and 6), presumably because of its smaller size and better membrane permeability. Finally, mHtt aggregation was significantly reduced in the

striatum region of 9-month-old YAC128 mice after 30-day ICV infusion with HQP09 compared with the control group of age-matched YAC128 mice infused with ACSF (Figure 7) without causing significant neuronal toxicity (Figure S5). Infusion with HQP09 also resulted in improvement of motor performance of YAC128 mice (Figure S4).

From these studies, we concluded that HQP09 constitutes a promising lead for developing HD therapy, especially in view of the fact that peptoids share favorable pharmacological characteristics such as resistance to degradation in vivo and good cell membrane and blood brain barrier permeability (Zuckermann and Kodadek, 2009). At present, peptoid technology has very limited application in the field of neuroscience and neurodegeneration. In a recent study, combinatorial peptoid library was used to identify diagnostically useful antibodies in a sera collected from Alzheimer's patients (Reddy et al., 2011). In another study two 3-mer peptoids were isolated as potential neuroprotective agents in a cell-based screen for inhibitors of glutamate-induced excitotoxicity (Montoliu et al., 2002). However, the target and the mechanism of action of those initial hits were not identified (Montoliu et al., 2002), which made further optimization difficult. In contrast, the target of HQP09 is known and structure-functional optimization can be easily performed using the competitive FP-based binding assay that we developed (Figure 3). The structures of resulting peptoids can be further optimized by taking advantage of recently solved crystal structure of Htt-17Q exon 1 fragment (Kim et al., 2009). The biological activities of generated leads could be easily validated using the mHtt aggregation assay (Figure 4), Ca^{2+} imaging/apoptosis assays with YAC128 MSN cultures (Figures 5 and 6), and in in vivo experiments with YAC128 mice (Figure 7). Our next goal is to proceed in HQP09 optimization and extend this technology to identify peptoids (and peptoids derivatives) that may be beneficial to other polyQ expansion disease models, such as SCA3 and SCA2. In future studies, we plan to test this hypothesis in experiments with SCA3-YAC84 or SCA2-58Q mouse models as we previously described (Chen et al., 2008; Liu et al., 2009).

EXPERIMENTAL PROCEDURES

Materials and Equipment

See Supplemental Experimental Procedures online.

Animals

All animal studies and surgical procedures were approved by the University of Texas Southwestern Medical Center Animal Care and Use Committee. YAC128 mice (FVBN/NJ background strain) (Slow et al., 2003) were obtained from Jackson Labs (Bar Harbor, ME). Pups were used for the preparation of MSNs cultures at postnatal days 0–2 and maintained as previously described (Tang et al., 2005). Adult 8–9 month old WT and YAC128 mice were used to test the efficacy of peptoids.

Generation of the Peptoid Library

The synthesis of the one-bead-one–compound peptoid library was accomplished using a standard combinatorial "split and pool" strategy in accordance with a previously published protocol (Alluri et al., 2003), and the resulting library consisted of 60,000 peptoids (beads). The detailed procedure of library synthesis is described in the Supplementary Methods.

Expression, Purification, and Biotinylation of Human Htt

A first exon (EX1) fragment of the human Htt protein (The Huntington's Disease Collaborative Research Group, 1993) (Met1-Gln66) containing 15 CAG repeats or 82 CAG repeats was amplified by polymerase chain reaction (PCR) and cloned into the pMAL vector with a modified 3A-linker as previously described (Kim et al., 2009). The maltose-binding protein (MBP)-Htt-N-15Q and MBP-Htt-N-82Q proteins were expressed in *Escherichia coli* BL21-RIL strain and affinity-purified on amylose resin as previously described (Kim et al., 2009). The MBP-Htt-N-82Q protein was labeled with biotin. For details, see Supplementary Methods.

Peptoid Library Screening

The *E. coli* lysates were prepared as described in Supplementary Methods, and all procedures were performed at 4°C. Approximately 60,000 TentaGel macrobeads (120 mg, manufacturer) of the synthesized peptoid library were swollen in Tris-buffered saline (50 mM Tris, pH 7.4, 150 mM NaCl) with 0.1% Tween 20 (TBST) for 1 hr. The beads were incubated with Binding Buffer (10 mg/ml *E. coli* lysate and 0.5% BSA in TBST) for 1 hr to block non-specific binding, and then incubated with MBP-Htt-N-82Q (200 nM) in Binding Buffer overnight. The unbound proteins were removed by washing twice with TBST. The washed beads were incubated with anti-MBP mouse IgG (1:1000, New England BioLabs, Ipswich, MA) in Binding Buffer for 2 hr and the unbound antibody was removed by several washes with TBST. The beads were incubated with 500 μl of 5 nM Qdot 655 goat anti-mouse IgG (Invitrogen, Eugene, OR) in Binding Buffer for 1.5 hr. Finally, after washing and removing unbound Qdot, the beads were visualized under an Olympus IX70 fluorescence microscope using an excitation wavelength of 410 nm. The blue beads with red Qdot circles were manually picked using pipette tips and pooled together. The Qdot was stripped off the target bound to the beads and re-probed with biotinylated bio-MBP-Htt-N-82Q protein and streptavidin-Qdot.

Hit Identification and Resynthesis of Peptoids

Each individual bead containing putative "hits" was heated at 90°C in 30 μl of 1% SDS in H_2O for 20 min, followed by three washes with phosphate-buffered saline (PBS) and three washes with water. The beads were added to a cartridge under stereo microscope (5x) and sequenced by Edman degradation (UT Southwestern Medical Center Chemistry Core). The peaks for each peptoid were compared with retention times of the 9 residues used to generate the screening library (Figure 1B). Selected peptoids were re-synthesized on the TentaGel beads using the same protocol used for the synthesis of the peptoid library. For binding studies and biological assays, the peptoids were synthesized on 4-methylbenzhydrylamine MBHA resin (Novabiochem, Darmstadt, Germany), chemically cleaved off the resin, and purified by high-performance liquid chromatography as described in Supplementary Methods.

In Vitro Binding Experiments

To prepare the $(QBP1)_2$ beads, 15 μg of streptavidin agarose beads (Sigma, St. Louis, MO) were saturated by 10 μg of Bio-$(QBP1)_2$ peptide in 500 μl TBST buffer at 4°C for 1 hr. The QBP1 beads were generated using similar procedure using Bio-QBP1 peptide. The beads were washed twice in TBST to remove unbound peptide and used in pull-down experiments. The HQP09 and RP01 peptoids were synthesized on Tentagel Macrobeads as described for library synthesis. Before binding experiments, 10 μl of each type of bead were blocked with 0.5% BSA in TBST buffer at 4°C for 1 hr. The MBP-Htt-N-82Q or MBP-Htt-N-15Q fusion proteins (4 μg each) were incubated overnight with the beads in 500 μl of 0.5% BSA (in TBST buffer). The beads were washed twice with TBST, heated at 100°C for 5 min in the gel-loading buffer, and analyzed by SDS-PAGE and western blotting with an anti-MBP monoclonal antibody (New England Biolabs, E8032). Full-length Atxn3–19Q and Atxn3–77Q proteins were expressed in Sf9 cells by baculovirus infection as previously described (Chen et al., 2008). The microsomes prepared from infected Sf9 cells were solubilized in 1% CHAPS, dialyzed in TBST buffer for 2 hr, and used in pull-down experiments. The precipitated samples were analyzed by western blotting with an anti-Atxn3 monoclonal antibody (Millipore MAB5360, Temecula, CA).

Fluorescence Polarization Assay

The fluoresceinated HQP09 peptoid was synthesized by reacting HQP09_G2 (Figure 3A) with fluorescein-5-maleimide (Thermo Scientific, #46130). The fluoresceinated HQP09 (5 nM) was incubated with indicated concentrations of BSA or MBP-Htt-N-82Q in the presence of 1.0 μM BSA in TBST (pH 7.4)

in a final volume of 100 μl on ice for 0.5 hr in the dark. The fluorescence polarization values were measured using Panvera Beacon 2000 instrument (Invitrogen). In competition experiments, HQP09 and all analogs were included in the binding reaction in a final concentration of 300 μM.

Aggregation Assays

The filter trap and western blotting assays were performed as previously described (Wacker et al., 2004). The aggregation of Htt53Q was initiated by the addition of PreScission Protease (4 unites/100 μg fusion protein, Amersham Biosciences/GE Healthcare, Piscataway, NJ) to purified GST-Htt53Q protein. After cleavage, the Htt53Q proteins (6 μM) were incubated in 3% DMSO, QBP1 peptide or peptoids (10 μM) in 20 mM Tris-HCl pH7.5, 150 mM KCl, 1 mM DTT at 37°C with shaking at 800 rpm. The 2 μg aliquots of Htt53Q were removed from the reaction, boiled in SDS-loading buffer, and applied to a nitrocellulose membrane (0.2 μm pore size, Schleicher & Schuell, Keene, NH) through a slot-blot manifold. After washing with SDS-Buffer by vacuum filtering, the membranes were incubated in blocking buffer and probed with the MW8 monoclonal antibody (gift from Paul Patterson) raised against the last eight amino acids of Htt exon 1 (AEEPLHRP) (Ko et al., 2001). The density of trapped Htt53Q aggregates was quantified by using Image J (NIH, Bethesda, MD). For western blotting analysis, the proteins and aggregates were separated by SDS-PAGE and analyzed with the MW8 antibody.

Atomic Force Microscopy

The tapping mode AFM images were collected on an Asylum Research MFP-3D™ atomic force microscope (Asylum Research, Santa Barbara, CA), with 120-μm-long oxide-sharpened silicon nitride V-shaped NP-S cantilevers (Veeco Instruments, Santa Barbara, CA). The samples were prepared and incubated for 24 hr as described for aggregation assays. Immediately before AFM experiments, the Htt53Q samples were diluted 20 times in the binding buffer and deposited on freshly cleaved mica surface. All images were captured in frame size of 10 × 10 μm, at a resolution of 1024 × 1024 pixels, and with a scanning rate of 1 Hz. The driving frequency of the oscillating tip is within the range of 8∼10 kHz. The captured images were flattened and plane-fitted in the second order before analysis. The number of particles with effective diameter larger than 100 nm was counted by using Image J.

Calcium Imaging and Apoptosis Experiments

Post-natal day 1–2 pups were collected and genotyped for YAC128 by PCR. Primary cultures of striatal MSN were established as before (Tang et al., 2005, 2007; Wu et al., 2006). Ca^{2+} imaging and apoptosis experiments were performed as we previously described (Tang et al., 2005, 2007; Wu et al., 2006). For treatments, HQP09, HQP09_9, and RP01 peptoids were added on DIV1 and DIV13 at a final concentration of 20 μM in both Ca^{2+} imaging and apoptosis experiments. See Supplementary Methods for details.

Peptoid Delivery in Mice

The peptoid HQP09 (100 μl total volume, 25 mg/ml in ACSF) or 100 μl ACSF was injected ICV to four groups of WT and YAC128 mice at 8–9 months old. The peptoids were delivered by Alzet microosmotic pump 1004 (Durect Corporation, Cupertino, CA), which was connected to a cannula via a catheter tube from the Brain Infusion Kit 3 (Durect Corporation). After the mice were anesthesized with a mixture of ketamine (120 mg/kg) and xylazine (16 mg/kg, UTSW ARC), the cannula was placed into the left lateral ventricle (anteroposterior: −0.3 mm; medium-line: −1 mm) using a Kopf (David Kopf, Tujunga, CA) stereotaxic instrument and fixed by glass ionomer luting cement (3M ESPE, St. Paul, MN). The Alzet pump was inserted subcutaneously in the back of the mice and the incision was closed by absorbable polyglycolic acid sutures.

Motor Coordination Assessments in Mice

The "beam-walk" test was used to assess motor coordination in mice as we described previously (Chen et al., 2008; Liu et al., 2009; Tang et al., 2007, 2009; Wang et al., 2010) using 11-mm, round plastic beam. The ratio of the latency for each individual mouse before and after ICV treatment was determined.

Immunohistochemistry

After treatments, mice were anesthetized with Euthasol and perfused transcardially first with 30 ml of PBS, then 50 ml of 4% paraformaldehyde (PFA) in PBS. All mice brains were post-fixed overnight at 4°C in PFA and equilibrated in 25% (w/v) sucrose in PBS. The brains of YAC128 mice were frozen in dry ice and sliced into 30-μm-thick coronal sections using a Leica SM 2000R sliding microtome (Bannockburn, IL). Six coronal sections that contain the striatum (in the range from +0.86 mm to +0.14 mm relative to bregma) were washed in PBS and blocked with mouse IgG (Vector Laboratories, Burlingame, CA) for 1 hr. Slices were then stained with EM48 monoclonal antibody (MAB5374, 1:250, Millipore) which was diluted in the M.O.M. (Vector Laboratories) working solution with 0.25% Triton X-100 overnight. After being washed twice in PBS, brain slices were incubated with goat anti-mouse IgG conjugated with AlexFluor 594 (1:500) for 2 hr and Neurotrace 500/525 for 1 hr (1:500, Invitrogen) at RT in the dark. The slices were washed twice in PBS and mounted on glass slides with Aqua Poly/Mount (Polysciences Inc, Warrington, PA). Images were collected with a Zeiss spectral laser confocal microscope using ZEN2009 software with excitation at 488 nm and 543 nm. The settings for acquiring photos were: frame size: 1024 × 1024; averaging number: 2; Z stack keeping 10 slides per view. Fifteen images per slice were collected from the middle part of the slices (20 μm thick) to the striatum. The confocal images were analyzed using MetaXpress (Molecular Devices, Sunnyvale, CA) to quantify the area containing aggregates and to determine the intensity of mutant Htt aggregation.

SUPPLEMENTAL INFORMATION

Supplemental Information includes five figures, two tables, and Supplemental Experimental Procedures and can be found with this article online at doi:10.1016/j.chembiol.2011.06.010.

ACKNOWLEDGMENTS

We express our appreciation for technical help and useful suggestions from the members of IB, PJM and TK laboratories. We thank Huraui Liu for help maintaining the YAC128 mouse colony and Leah Benson for administrative assistance. This work was supported by CHDI foundation (I.B. and P.J.M.), the UT Southwestern Center for Proteomics Research (T.K.), and the US National Institutes of Health (R01NS056224 and 3R01NS056224-02S1 to I.B., R01NS054753 to P.J.M., and NO1-HV-28185 to T.K.).

Received: March 22, 2011
Revised: May 26, 2011
Accepted: June 22, 2011
Published: September 22, 2011

REFERENCES

Alluri, P.G., Reddy, M.M., Bachhawat-Sikder, K., Olivos, H.J., and Kodadek, T. (2003). Isolation of protein ligands from large peptoid libraries. J. Am. Chem. Soc. *125*, 13995–14004.

Alluri, P., Liu, B., Yu, P., Xiao, X., and Kodadek, T. (2006). Isolation and characterization of coactivator-binding peptoids from a combinatorial library. Mol. Biosyst. *2*, 568–579.

Benn, C.L., Sun, T., Sadri-Vakili, G., McFarland, K.N., DiRocco, D.P., Yohrling, G.J., Clark, T.W., Bouzou, B., and Cha, J.H. (2008). Huntingtin modulates transcription, occupies gene promoters in vivo, and binds directly to DNA in a polyglutamine-dependent manner. J. Neurosci. *28*, 10720–10733.

Bezprozvanny, I. (2009). Calcium signaling and neurodegenerative diseases. Trends Mol. Med. *15*, 89–100.

Chaturvedi, R.K., and Beal, M.F. (2008). Mitochondrial approaches for neuroprotection. Ann. N Y Acad. Sci. *1147*, 395–412.

Chen, X., Tang, T.S., Tu, H., Nelson, O., Pook, M., Hammer, R., Nukina, N., and Bezprozvanny, I. (2008). Deranged calcium signaling and neurodegeneration in spinocerebellar ataxia type 3. J. Neurosci. *28*, 12713–12724.

Chopra, V., Fox, J.H., Lieberman, G., Dorsey, K., Matson, W., Waldmeier, P., Housman, D.E., Kazantsev, A., Young, A.B., and Hersch, S. (2007).

A small-molecule therapeutic lead for Huntington's disease: preclinical pharmacology and efficacy of C2-8 in the R6/2 transgenic mouse. Proc. Natl. Acad. Sci. USA *104*, 16685–16689.

Colby, D.W., Chu, Y., Cassady, J.P., Duennwald, M., Zazulak, H., Webster, J.M., Messer, A., Lindquist, S., Ingram, V.M., and Wittrup, K.D. (2004). Potent inhibition of huntingtin aggregation and cytotoxicity by a disulfide bond-free single-domain intracellular antibody. Proc. Natl. Acad. Sci. USA *101*, 17616–17621.

Ehrnhoefer, D.E., Duennwald, M., Markovic, P., Wacker, J.L., Engemann, S., Roark, M., Legleiter, J., Marsh, J.L., Thompson, L.M., Lindquist, S., et al. (2006). Green tea (-)-epigallocatechin-gallate modulates early events in huntingtin misfolding and reduces toxicity in Huntington's disease models. Hum. Mol. Genet. *15*, 2743–2751.

Gusella, J.F., and MacDonald, M.E. (2000). Molecular genetics: unmasking polyglutamine triggers in neurodegenerative disease. Nat. Rev. Neurosci. *1*, 109–115.

Hamuro, L., Zhang, G., Tucker, T.J., Self, C., Strittmatter, W.J., and Burke, J.R. (2007). Optimization of a polyglutamine aggregation inhibitor peptide (QBP1) using a thioflavin T fluorescence assay. Assay Drug Dev. Technol. *5*, 629–636.

Hara, T., Durell, S.R., Myers, M.C., and Appella, D.H. (2006). Probing the structural requirements of peptoids that inhibit HDM2-p53 interactions. J. Am. Chem. Soc. *128*, 1995–2004.

Harper, S.Q., Staber, P.D., He, X., Eliason, S.L., Martins, I.H., Mao, Q., Yang, L., Kotin, R.M., Paulson, H.L., and Davidson, B.L. (2005). RNA interference improves motor and neuropathological abnormalities in a Huntington's disease mouse model. Proc. Natl. Acad. Sci. USA *102*, 5820–5825.

Heiser, V., Engemann, S., Bröcker, W., Dunkel, I., Boeddrich, A., Waelter, S., Nordhoff, E., Lurz, R., Schugardt, N., Rautenberg, S., et al. (2002). Identification of benzothiazoles as potential polyglutamine aggregation inhibitors of Huntington's disease by using an automated filter retardation assay. Proc. Natl. Acad. Sci. USA *99* (*Suppl 4*), 16400–16406.

Hershberger, S.J., Lee, S.G., and Chmielewski, J. (2007). Scaffolds for blocking protein-protein interactions. Curr. Top. Med. Chem. *7*, 928–942.

Hu, J., Matsui, M., Gagnon, K.T., Schwartz, J.C., Gabillet, S., Arar, K., Wu, J., Bezprozvanny, I., and Corey, D.R. (2009). Allele-specific silencing of mutant huntingtin and ataxin-3 genes by targeting expanded CAG repeats in mRNAs. Nat. Biotechnol. *27*, 478–484.

Khoshnan, A., Ko, J., and Patterson, P.H. (2002). Effects of intracellular expression of anti-huntingtin antibodies of various specificities on mutant huntingtin aggregation and toxicity. Proc. Natl. Acad. Sci. USA *99*, 1002–1007.

Kim, M.W., Chelliah, Y., Kim, S.W., Otwinowski, Z., and Bezprozvanny, I. (2009). Secondary structure of Huntingtin amino-terminal region. Structure *17*, 1205–1212.

Ko, J., Ou, S., and Patterson, P.H. (2001). New anti-huntingtin monoclonal antibodies: implications for huntingtin conformation and its binding proteins. Brain Res. Bull. *56*, 319–329.

Lecerf, J.M., Shirley, T.L., Zhu, Q., Kazantsev, A., Amersdorfer, P., Housman, D.E., Messer, A., and Huston, J.S. (2001). Human single-chain Fv intrabodies counteract in situ huntingtin aggregation in cellular models of Huntington's disease. Proc. Natl. Acad. Sci. USA *98*, 4764–4769.

Lim, H.S., Archer, C.T., and Kodadek, T. (2007). Identification of a peptoid inhibitor of the proteasome 19S regulatory particle. J. Am. Chem. Soc. *129*, 7750–7751.

Liu, B., Alluri, P.G., Yu, P., and Kodadek, T. (2005). A potent transactivation domain mimic with activity in living cells. J. Am. Chem. Soc. *127*, 8254–8255.

Liu, J., Tang, T.S., Tu, H., Nelson, O., Herndon, E., Huynh, D.P., Pulst, S.M., and Bezprozvanny, I. (2009). Deranged calcium signaling and neurodegeneration in spinocerebellar ataxia type 2. J. Neurosci. *29*, 9148–9162.

Montoliu, C., Humet, M., Canales, J.J., Burda, J., Planells-Cases, R., Sánchez-Baeza, F., Carbonell, T., Pérez-Payá, E., Messeguer, A., Ferrer-Montiel, A., and Felipo, V. (2002). Prevention of in vivo excitotoxicity by a family of trialkylglycines, a novel class of neuroprotectants. J. Pharmacol. Exp. Ther. *301*, 29–36.

Nagai, Y., Tucker, T., Ren, H., Kenan, D.J., Henderson, B.S., Keene, J.D., Strittmatter, W.J., and Burke, J.R. (2000). Inhibition of polyglutamine protein aggregation and cell death by novel peptides identified by phage display screening. J. Biol. Chem. *275*, 10437–10442.

Nagai, Y., Fujikake, N., Ohno, K., Higashiyama, H., Popiel, H.A., Rahadian, J., Yamaguchi, M., Strittmatter, W.J., Burke, J.R., and Toda, T. (2003). Prevention of polyglutamine oligomerization and neurodegeneration by the peptide inhibitor QBP1 in Drosophila. Hum. Mol. Genet. *12*, 1253–1259.

Nagai, Y., Inui, T., Popiel, H.A., Fujikake, N., Hasegawa, K., Urade, Y., Goto, Y., Naiki, H., and Toda, T. (2007). A toxic monomeric conformer of the polyglutamine protein. Nat. Struct. Mol. Biol. *14*, 332–340.

Popiel, H.A., Nagai, Y., Fujikake, N., and Toda, T. (2007). Protein transduction domain-mediated delivery of QBP1 suppresses polyglutamine-induced neurodegeneration in vivo. Mol. Ther. *15*, 303–309.

Popiel, H.A., Nagai, Y., Fujikake, N., and Toda, T. (2009). Delivery of the aggregate inhibitor peptide QBP1 into the mouse brain using PTDs and its therapeutic effect on polyglutamine disease mice. Neurosci. Lett. *449*, 87–92.

Reddy, M.M., Wilson, R., Wilson, J., Connell, S., Gocke, A., Hynan, L., German, D., and Kodadek, T. (2011). Identification of candidate IgG biomarkers for Alzheimer's disease via combinatorial library screening. Cell *144*, 132–142.

Sánchez, I., Mahlke, C., and Yuan, J. (2003). Pivotal role of oligomerization in expanded polyglutamine neurodegenerative disorders. Nature *421*, 373–379.

Shao, J., and Diamond, M.I. (2007). Polyglutamine diseases: emerging concepts in pathogenesis and therapy. Hum. Mol. Genet. *16*, *Spec No. 2*, R115-R123.

Simon, R.J., Kania, R.S., Zuckermann, R.N., Huebner, V.D., Jewell, D.A., Banville, S., Ng, S., Wang, L., Rosenberg, S., Marlowe, C.K., et al. (1992). Peptoids: a modular approach to drug discovery. Proc. Natl. Acad. Sci. USA *89*, 9367–9371.

Simpson, L.S., Burdine, L., Dutta, A.K., Feranchak, A.P., and Kodadek, T. (2009). Selective toxin sequestrants for the treatment of bacterial infections. J. Am. Chem. Soc. *131*, 5760–5762.

Slow, E.J., van Raamsdonk, J., Rogers, D., Coleman, S.H., Graham, R.K., Deng, Y., Oh, R., Bissada, N., Hossain, S.M., Yang, Y.Z., et al. (2003). Selective striatal neuronal loss in a YAC128 mouse model of Huntington disease. Hum. Mol. Genet. *12*, 1555–1567.

Stevanin, G., Dürr, A., and Brice, A. (2000). Clinical and molecular advances in autosomal dominant cerebellar ataxias: from genotype to phenotype and physiopathology. Eur. J. Hum. Genet. *8*, 4–18.

Tang, T.S., Slow, E., Lupu, V., Stavrovskaya, I.G., Sugimori, M., Llinás, R., Kristal, B.S., Hayden, M.R., and Bezprozvanny, I. (2005). Disturbed Ca2+ signaling and apoptosis of medium spiny neurons in Huntington's disease. Proc. Natl. Acad. Sci. USA *102*, 2602–2607.

Tang, T.S., Chen, X., Liu, J., and Bezprozvanny, I. (2007). Dopaminergic signaling and striatal neurodegeneration in Huntington's disease. J. Neurosci. *27*, 7899–7910.

Tang, T.S., Guo, C., Wang, H., Chen, X., and Bezprozvanny, I. (2009). Neuroprotective effects of inositol 1,4,5-trisphosphate receptor C-terminal fragment in a Huntington's disease mouse model. J. Neurosci. *29*, 1257–1266.

The Huntington's Disease Collaborative Research Group. (1993). A novel gene containing a trinucleotide repeat that is expanded and unstable on Huntington's disease chromosomes. Cell *72*, 971–983.

Udugamasooriya, D.G., Dineen, S.P., Brekken, R.A., and Kodadek, T. (2008a). A peptoid "antibody surrogate" that antagonizes VEGF receptor 2 activity. J. Am. Chem. Soc. *130*, 5744–5752.

Udugamasooriya, D.G., Dunham, G., Ritchie, C., Brekken, R.A., and Kodadek, T. (2008b). The pharmacophore of a peptoid VEGF receptor 2 antagonist includes both side chain and main chain residues. Bioorg. Med. Chem. Lett. *18*, 5892–5894.

Vonsattel, J.P., and DiFiglia, M. (1998). Huntington disease. J. Neuropathol. Exp. Neurol. *57*, 369–384.

Vonsattel, J.P., Myers, R.H., Stevens, T.J., Ferrante, R.J., Bird, E.D., and Richardson, E.P., Jr. (1985). Neuropathological classification of Huntington's disease. J. Neuropathol. Exp. Neurol. *44*, 559–577.

Wacker, J.L., Zareie, M.H., Fong, H., Sarikaya, M., and Muchowski, P.J. (2004). Hsp70 and Hsp40 attenuate formation of spherical and annular polyglutamine oligomers by partitioning monomer. Nat. Struct. Mol. Biol. *11*, 1215–1222.

Wang, J., Gines, S., MacDonald, M.E., and Gusella, J.F. (2005). Reversal of a full-length mutant huntingtin neuronal cell phenotype by chemical inhibitors of polyglutamine-mediated aggregation. BMC Neurosci. *6*, 1.

Wang, J., Wang, C.E., Orr, A., Tydlacka, S., Li, S.H., and Li, X.J. (2008). Impaired ubiquitin-proteasome system activity in the synapses of Huntington's disease mice. J. Cell Biol. *180*, 1177–1189.

Wang, H., Chen, X., Li, Y., Tang, T.S., and Bezprozvanny, I. (2010). Tetrabenazine is neuroprotective in Huntington's disease mice. Mol. Neurodegener. *5*, 18.

Warrick, J.M., Chan, H.Y., Gray-Board, G.L., Chai, Y., Paulson, H.L., and Bonini, N.M. (1999). Suppression of polyglutamine-mediated neurodegeneration in Drosophila by the molecular chaperone HSP70. Nat. Genet. *23*, 425–428.

Wolfgang, W.J., Miller, T.W., Webster, J.M., Huston, J.S., Thompson, L.M., Marsh, J.L., and Messer, A. (2005). Suppression of Huntington's disease pathology in Drosophila by human single-chain Fv antibodies. Proc. Natl. Acad. Sci. USA *102*, 11563–11568.

Wu, J., Tang, T., and Bezprozvanny, I. (2006). Evaluation of clinically relevant glutamate pathway inhibitors in in vitro model of Huntington's disease. Neurosci. Lett. *407*, 219–223.

Wu, J., Li, Q., and Bezprozvanny, I. (2008). Evaluation of Dimebon in cellular model of Huntington's disease. Mol. Neurodegener. *3*, 15.

Wu, J., Jeong, H.K., Bulin, S.E., Kwon, S.W., Park, J.H., and Bezprozvanny, I. (2009). Ginsenosides protect striatal neurons in a cellular model of Huntington's disease. J. Neurosci. Res. *87*, 1904–1912.

Wu, J., Shih, H.P., Vigont, V., Hrdlicka, L., Diggins, L., Singh, C., Mahoney, M., Chesworth, R., Shapiro, G., Zimina, O., et al. (2011). Neuronal store-operated calcium entry pathway as a novel therapeutic target for Huntington's disease treatment. Chem. Biol. *18*, 777–793.

Wyttenbach, A., Sauvageot, O., Carmichael, J., Diaz-Latoud, C., Arrigo, A.P., and Rubinsztein, D.C. (2002). Heat shock protein 27 prevents cellular polyglutamine toxicity and suppresses the increase of reactive oxygen species caused by huntingtin. Hum. Mol. Genet. *11*, 1137–1151.

Xia, H., Mao, Q., Eliason, S.L., Harper, S.Q., Martins, I.H., Orr, H.T., Paulson, H.L., Yang, L., Kotin, R.M., and Davidson, B.L. (2004). RNAi suppresses polyglutamine-induced neurodegeneration in a model of spinocerebellar ataxia. Nat. Med. *10*, 816–820.

Xiao, X., Yu, P., Lim, H.S., Sikder, D., and Kodadek, T. (2007). A cell-permeable synthetic transcription factor mimic. Angew. Chem. Int. Ed. Engl. *46*, 2865–2868.

Zhang, X., Smith, D.L., Meriin, A.B., Engemann, S., Russel, D.E., Roark, M., Washington, S.L., Maxwell, M.M., Marsh, J.L., Thompson, L.M., et al. (2005). A potent small molecule inhibits polyglutamine aggregation in Huntington's disease neurons and suppresses neurodegeneration in vivo. Proc. Natl. Acad. Sci. USA *102*, 892–897.

Zuckermann, R.N., and Kodadek, T. (2009). Peptoids as potential therapeutics. Curr. Opin. Mol. Ther. *11*, 299–307.